Normalization is a general neural mechanism for context-dependent decision making

Kenway Louie[1], Mel W. Khaw, and Paul W. Glimcher

Center for Neural Science, New York University, New York, NY 10003

Edited by William T. Newsome, Stanford University, Stanford, CA, and approved March 1, 2013 (received for review October 14, 2012)

Understanding the neural code is critical to linking brain and behavior. In sensory systems, divisive normalization seems to be a canonical neural computation, observed in areas ranging from retina to cortex and mediating processes including contrast adaptation, surround suppression, visual attention, and multisensory integration. Recent electrophysiological studies have extended these insights beyond the sensory domain, demonstrating an analogous algorithm for the value signals that guide decision making, but the effects of normalization on choice behavior are unknown. Here, we show that choice models using normalization generate significant (and classically irrational) choice phenomena driven by either the value or number of alternative options. In value-guided choice experiments, both monkey and human choosers show novel context-dependent behavior consistent with normalization. These findings suggest that the neural mechanism of value coding critically influences stochastic choice behavior and provide a generalizable quantitative framework for examining context effects in decision making.

context dependence | divisive normalization | neural coding | neuroeconomics | reward

A fundamental question in neuroscience is how the brain represents behaviorally relevant variables. Neural coding is governed by a small number of canonical computations implemented in diverse circuits and mechanisms, a prominent example being divisive normalization, in which the initial input-driven activity of a neuron is divided by the summed activity of a large pool of neighboring neurons. Originally proposed to explain nonlinear responses in primary visual cortex (1), divisive normalization has been widely observed in sensory systems and characterizes responses including contrast gain control in the retina and thalamus (2, 3), surround suppression in the middle temporal area (4, 5), ventral stream responses to multiple objects (6), and gain control in auditory cortex (7). Normalization also explains neural activity underlying higher-order processes such as multisensory integration (8) and visual attention (9). This ubiquity may reflect the role of normalization in generating normative coding efficiency via processes such as gain control, feature invariance, and redundancy reduction (10–12).

Recent neurophysiological evidence shows that such normalization processes extend beyond sensory areas to higher-order cortical areas involved in decision making. In parietal and premotor cortex, neurons specifying individual actions are strongly modulated by the value of those actions (13–16). Importantly, this value representation is encoded in a normalized form: Firing rates are increased by increases in the value of the represented action and suppressed by increases in the value of alternative actions (17–19). Such normalization, however, introduces an inherent context dependence in neural coding. In the visual system, normalization underlies contextual modulation of activity by extrareceptive field stimuli, for example surround suppression in visual cortical neurons (12, 20). In decision-related areas, normalization produces an analogous context dependence, where the neural representation of the value of an option is explicitly dependent on the value of other available alternatives. Although the nature of value representation is closely tied to the decision process, the behavioral implications of value normalization are unknown.

Here we develop a model of decision making derived directly from neurophysiologically observed value normalization (17) and show that it predicts a unique form of context-dependent choice behavior. A fundamental assumption of many traditional rational theories of choice is that the context-independent value of options guides decision making (21, 22); how a chooser decides between any two options should not depend on the number or quality of other options, a property known as independence of irrelevant alternatives, or IIA (23). However, at an empirical level it is known that context can profoundly affect choice behavior in species ranging from insects to birds to humans (24–28). Various explanations have been proposed for specific context effects, but to date no general model rooted in specific physiological data exists for context-dependent choice.

We show here that the normalization model predicts significant context-dependent rationality violations in computational simulations, driven by normalized scaling of value-coding neural activity. These simulations provide a quantitative examination of qualitative predictions about the effects of normalization on decision making (17, 29). Furthermore, we examine human and monkey behavior under conditions in which the model specifically predicts context-driven distortions of choice behavior. These findings demonstrate a direct link between divisive normalization and behavior and suggest that normalization is a fundamental feature of cortical computation beyond the sensory domain.

Results

Forms of Value Representation. Value-related neural activity has been observed in multiple brain areas underlying decision making, for example in areas linked to action selection. Such value coding is presumably critical to the decision process, providing the appropriate decision values for action selection. Many initial studies have interpreted this activity in terms of an absolute value code, for example:

$$\mu_i = K \cdot V_i, \qquad [1]$$

where the mean firing rate representing the value of option i is postulated to be a function of that option value alone. However, recent experiments suggest that these brain areas, including portions of premotor and parietal cortex, use a relative value code (17–19). We have recently demonstrated that relative value representation in parietal cortex is specifically implemented by the classic divisive normalization algorithm (17), in which each option value is transformed into a mean firing rate:

Author contributions: K.L., M.W.K., and P.W.G. designed research; K.L. and M.W.K. performed research; K.L. analyzed data; and K.L. and P.W.G. wrote the paper.

The authors declare no conflict of interest.

This article is a PNAS Direct Submission.

[1]To whom correspondence should be addressed. E-mail: klouie@cns.nyu.edu.

This article contains supporting information online at www.pnas.org/lookup/suppl/doi:10.1073/pnas.1217854110/-/DCSupplemental.

$$\mu_i = K\frac{V_i}{\sigma_H + \sum_j wV_j}, \quad [2]$$

where V_i is the value of the option under consideration, the index j is summed over all available options, and the parameters K, σ_H, and w represent gain, semisaturation, and weight terms, respectively. The critical feature of this representation is the presence of all option values in the denominator, which mediates the relative nature of the value coding.

Model of Normalized Value Coding and Choice. A fundamental prediction of many rational theories of choice is that the relative preference of a chooser between any two options should be unaffected by choice context. A prominent example is the choice axiom of Luce, an instantiation of IIA (23). This requires that the ratio of stochastic choice probabilities for two given, or target, options (p_1/p_2) should be independent of the presence or value of a third, or distracter, option. Our simulations reveal, however, that the combination of normalized value coding and variability alone produces context-dependent choice behavior.

We modeled stochastic choice behavior with a simple algorithmic simulation comprising three components: value representation to transform each option value into a firing rate, stochastic variability to model noise in the coding process, and option selection to implement choice (Fig. 1*A*). For each option i, a mean firing rate μ_i was calculated from the option value and the values of other alternatives using Eq. **2**, thus implementing normalization. Note that because value is quantified in arbitrary units, the gain term K was set to reproduce realistic firing rates [~75 spikes per second (sp/s)]. For simplicity, the semisaturation and weight terms were set to standard fixed values (*Materials and Methods*).

To introduce structured trial-to-trial variability into the model, we added two forms of noise to each mean firing rate: a fixed noise term (ε_f), drawn from a zero-mean Gaussian distribution with fixed variance σ^2_{fixed}, and a mean-scaled noise term (ε_s), a class of noise commonly observed in cortical neurons that increases as mean firing rate increases (30, 31). Mean-scaled noise was drawn from a zero-mean Gaussian distribution with variance $S\mu_i$, where the parameter S controls the degree of mean scaling. Both types of noise were included to avoid assumptions about the specific form of variability; the magnitude of each term was varied independently to examine their relative contribution to model behavior (*SI Materials and Methods*). In each simulated trial, option selection was implemented by simply choosing the option with the highest postnoise activity in that trial. This procedure produces stochastic choice governed by the values of the offered options and the noise terms.

To demonstrate the critical nature of value coding representations, we show in Fig. 1*B* example choice simulations under either absolute or normalized value coding. We use the term "distracter" to denote a low-valued alternative that is eligible for selection; the critical issue is how distracter value affects relative target choice. In a traditional absolute value representation, relative preference between two fixed target options (V_1 = 150 and V_2 = 140, arbitrary units) remains constant as distracter value increases ($V_3 = 0$, $p_1/p_2 = 53.3$, bootstrap confidence interval [CI], [51.2, 55.8]; $V_3 = 120$, $p_1/p_2 = 52.9$, bootstrap CI [50.5, 55.3]). In a relative value representation, however, the mean firing rate of each option depends on the values of the other options. As distracter value (red) increases, divisive scaling decreases the distance between the target option firing rates (black and blue). The resulting increase in overlap between firing rate distributions decreases the relative preference of the chooser for the better target option ($V_3 = 0$, $p_1/p_2 = 51.7$, bootstrap CI [49.3, 54.0]; $V_3 = 120$, $p_1/p_2 = 15.8$, bootstrap CI [15.3, 16.2]).

Examined as a function of distracter value, normalized value coding produces a consistent decrease in relative target choice (p_1/p_2) that is absent under absolute value coding (Fig. 1*C*). Notably, a second type of context dependence emerges in both value representations when distracter values approach the target values (black and blue triangles): Increasing the value of the distracter increases the relative preference of the model for the better target option. This effect is driven by choices captured by the distracter option, which selectively competes with the lower-valued target option. Thus, under normalization context dependence is biphasic: Effective choice consistently decreases until distracter competition counteracts the effect of divisive scaling and offsets the normalization-induced decrease in relative target preference.

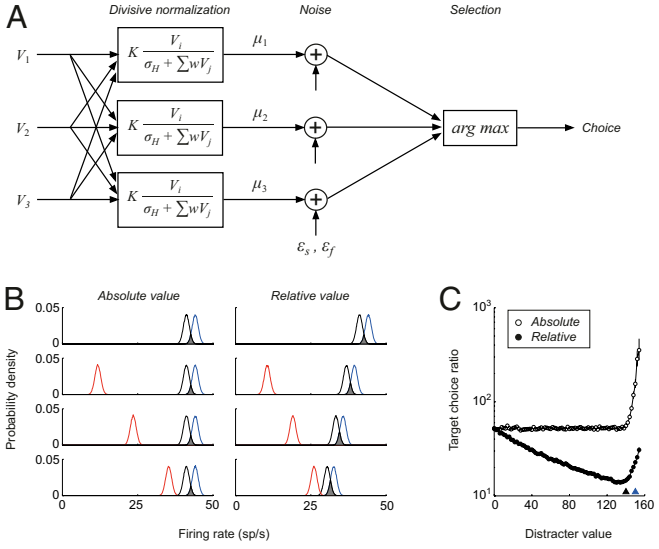

Fig. 1. Model of normalized value coding in stochastic choice. (*A*) Structure of the trinary-choice model. Value inputs (V_1,V_2, and V_3) were converted into mean firing rates (μ) representing each choice option and variability was introduced as noise terms added to the mean firing rates. In a given trial, the option with the maximum firing rate was designated as the chosen option. (*B*) Example difference between absolute and relative value-coding representations. Each curve shows the probability density function of the neural activity associated with one of three choice options. Under relative value coding, increasing distracter value (red) reduces the distance between target option distributions and decreases the relative choice ratio for the better target. Relative value parameter settings: K = 100, σ_H = 50, w = 1, σ_{fixed} = 1, S = 0. (*C*) Two forms of context dependence in stochastic choice behavior. Points show relative choice ratio between two targets (V_1 = 150 and V_2 = 140, arbitrary units) as a function of distracter value under absolute or relative value coding (error bars, bootstrap 95% CI).

Context Dependence in Simulated Choice Behavior. To examine trinary-choice behavior in detail, we simulated choice while varying both target value differences and distracter value under a range of noise parameters. Fig. 2*A* shows example data for a specific set of noise parameters ($\sigma_{fixed} = 8$, $S = 0$). In this simplex plot, each point represents how the average choice behavior for a given set of value conditions is divided between the three options, color-coded by distracter value (probability for a given option increases linearly with distance to its vertex). Notably, choice behavior as a function of distracter value for a given pair of target values (blue lines) differs markedly from the constant relative preference assumption (straight gray lines) of rational choice theory (23).

Fig. 2*B* summarizes this data as relative choice probabilities between the two targets, segregated by distracter value. In contrast to the constancy of relative preference predicted by IIA, these stochastic choice curves are shallower at higher distracter values. To quantify this stochasticity, we computed for each choice function the average efficiency (E), which ranges from 0.5 (random chooser) to 1 (perfect chooser) and varies inversely with stochasticity. Consistent with the previous example, the

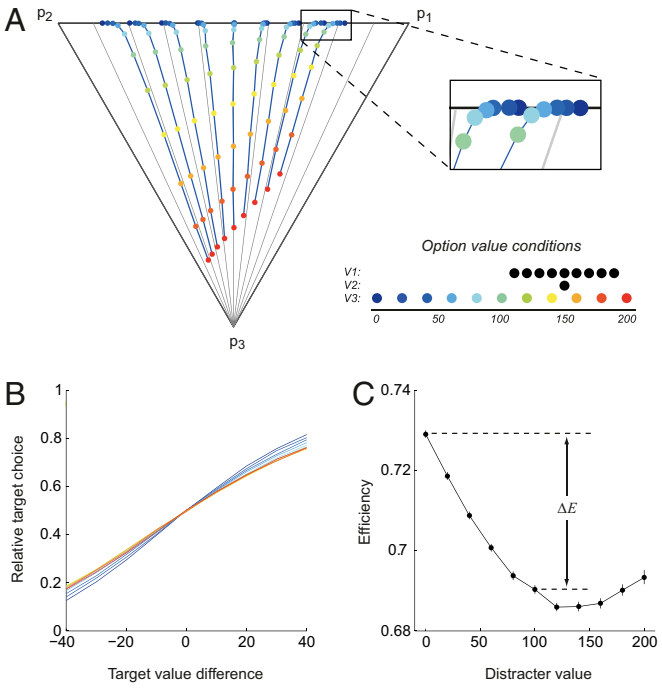

Fig. 2. Relative value coding generates context dependence in model choice behavior. (*A*) Example trinary-choice behavior. Each point in the simplex plot represents average choice behavior for a given triplet of value conditions, color-coded by distracter value (V_3). The choice probability of a given option is represented by the linear distance between its associated vertex and the opposite edge; for example, a point at the bottom vertex would represent 100% choice of option 3 ($p_1 = 0$, $p_2 = 0$, $p_3 = 1$) and a point in the midpoint of the top edge would represent 0% choice of option 3 ($p_1 = 0.5$, $p_2 = 0.5$, $p_3 = 0$). The legend shows the different value conditions, with each trial using a single value triplet (V_1, V_2, and V_3). Choice behavior under fixed target-value pairs (V_1 and V_2) are connected with blue lines and deviate markedly from the linear constant relative ratio lines predicted by rational-choice theory (gray lines). Example simulation parameters: $K = 100$, $\sigma_H = 50$, $w = 1$, $\sigma_{fixed} = 8$, $S = 0$. (*B*) Context-dependent relative target choice functions. Lines are color-coded by distracter value, as in *A*. (*C*) Relative target choice efficiency plotted as a function of distracter value. Efficiency is defined as the average choice probability for the better target across all target-value differences, a quantity that varies inversely with stochasticity. To quantify the normalization-driven context dependence, we measured the decrement in efficiency ($-\Delta E$) between $V_3 = 0$ and $V_3 = 100$.

effect of distracter value on efficiency is biphasic (Fig. 2*C*). Importantly, the primary normalization-driven decrease in choice efficiency persists across a broad range of noise levels (*SI Results* and Fig. S1) and normalization parameters (*SI Results* and Fig. S2).

Because normalized value coding incorporates the value of all available alternatives in the suppressive term, this mechanism should also generalize to set-size context effects. In simulations with target options and a varying number of low-valued distracters, we found that relative choice behavior between targets consistently decreases as the number of distracters increases (Fig. S3). Notably, set-size-driven context effects are larger than those seen in trinary choice because larger numbers of small-valued distracters increase the overall divisive scaling term without directly competing for selection.

Context Dependence in Monkey Choice Behavior. To test the predictions of the normalization model in empirical choice behavior, we examined monkey decision making in a simple trinary-choice task. Sessions were conducted in a block design; in each block, monkeys first learned the value associated with each of three different locations presented individually in instructed trials. In subsequent choice trials, the animals were presented with cues in the three locations simultaneously and were free to choose their preferred option. Both the target configuration and the value assignments were chosen randomly for each block (two monkeys, 598 blocks). Consistent with value-guided decision making, the monkeys distributed their choices according to the reward magnitudes ($p_{high\text{-}target} = 69.3\%$, $p_{low\text{-}target} = 27.0\%$, and $p_{distracter} = 3.7\%$, excluding trials where the two targets were of equal value).

To quantify context dependence, we examined choice behavior between two high-value targets at two different distracter values (Fig. 3). Strong value dependence was observed in the relative choice behavior between targets, as evident in logistic functions fit to the choice data and the difference between the values of the two targets (logistic slope parameters: Monkey W, $\alpha = 0.039$, 95% CI [0.036 0.043]; Monkey B, $\alpha = 0.061$, 95% CI [0.058 0.064]). More importantly, although the distracter was almost never chosen, its value had a strong effect on choice. In both monkeys, relative choice curves were steeper in the presence of a low- (Monkey W, $\alpha = 0.055$, 95% CI [0.050 0.060]; Monkey B, $\alpha = 0.080$, 95% CI [0.074 0.085]) versus a high-value distracter (Monkey W, $\alpha = 0.025$, 95% CI [0.020 0.029]; Monkey B, $\alpha = 0.046$, 95% CI [0.042 0.050]). Thus, the magnitude of a low-value distracter, an option that was essentially never chosen, nevertheless profoundly affects the efficiency of choice behavior. This effect resulted in a significant decrement in reward outcome: On average, at the largest value differences, the rate of correct decisions decreased from 84.4 to 69.1% (pooled data; $P << 0.001$, binomial proportion test).

Context Dependence in Human Choice Behavior. To date, examples of context dependence in the human literature primarily involve higher-order complexities in the decision process, such as the relative weighting of different option attributes. However, the normalization model suggests that context dependence can arise out of the fundamental coding mechanism of valuation itself. To test this hypothesis, we examined choice behavior in human subjects performing a two-stage valuation and choice task involving common snack-food items (Fig. 4*A*). In each bid trial, subjects viewed a single item and reported their maximum willingness to pay ($0–$4). If implemented, realization of one of these trials was conducted at the end of the experiment via an auction procedure designed to elicit subjects' true valuations (32) (Becker–DeGroot–Marschak auction, *SI Materials and Methods*). Subjects completed 60 bid trials with two repetitions for each of 30 items. Consistent with an elicitation of stable underlying valuations, individual item bids were strongly correlated across repetitions, as shown for an example subject (Fig. 4*B*; $r = 0.96$, $P = 1.62 \times 10^{-17}$) and quantified across the population (mean correlation $r = 0.87$; $P = 3.13 \times 10^{-36}$, t test).

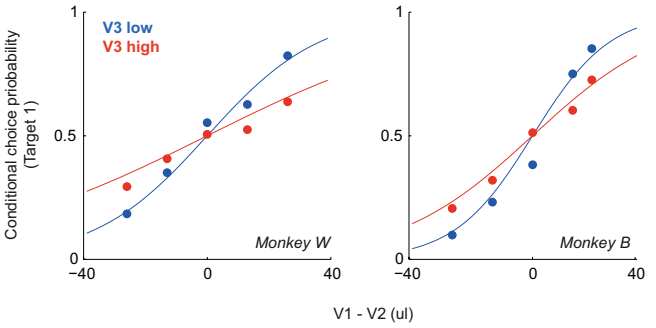

Fig. 3. Context dependence in monkey value-guided choice. Context-dependent behavior in a trinary-choice task. Points show average relative choice behavior between the two high-value target options in the presence of a low- (blue) or high- (red) value distracter. Curves plot logistic functions fit to the conditional choice data (either target chosen).

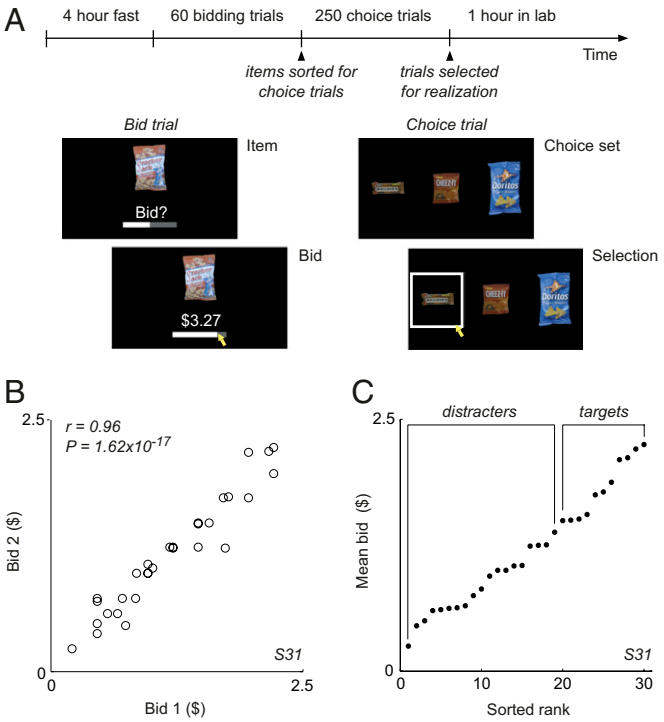

Fig. 4. Human choice behavior experiment. (*A*) Trinary-choice task. In each bid trial, subjects indicated the maximum price they would pay for a snack-food item. Subjects completed two bid trials for each of 30 food items. In each choice trial, subjects were presented with three food items and selected the one they most preferred. (*B*) Example bid data. Consistent with a stable valuation, subjects' bids for individual items were highly correlated across repetitions (example subject: $r = 0.96$, $P = 1.62 \times 10^{-17}$; population: mean $r = 0.87$, $P = 3.31 \times 10^{-36}$, t test). (*C*) Example bid distribution and choice-set construction. The 10 highest-valued items were assigned to be target items; 10 distracter items were sampled evenly from the 20 lowest-valued items.

We examined in subsequent choice trials how trinary-choice behavior depended on distracter valuations. For each subject, we selected a subset of 10 high-value items and 10 low-value items based on their individual mean valuations (targets and distracters, respectively; Fig. 4*C*). We then constructed 250 different trinary-choice sets pairing a range of single distracters with different target pairs, allowing us to examine how distracter value modulates choice efficiency. Consistent with value-guided decision making, overall choice behavior was governed by the values extracted from bid trials (population choice probabilities: high-value target 60.5%, low-value target 33.3%, and distracter 6.2%).

To examine context dependence across the subject population, we normalized distracter value relative to the target pair with a metric that ranges from 0 (small value) to 1 (large value). As predicted by the normalization model, relative choice of the better target consistently decreased as distracter value increased (Fig. 5*A*), with strong correlation between conditional choice probability and normalized distracter value ($r = -0.80$, $P = 0.006$). This effect exists across the population of subjects, as was evident when we examined individual conditional target choice under conditions of low versus high distracter value (Fig. 5*B*; mean difference in target choice 0.064, $P = 0.0019$, t test).

To examine this effect parametrically, we performed a generalized linear regression of the form

$$\eta = \beta_0 + \beta_1 V_1 + \beta_1 V_2 + \beta_3 normV_3,$$

quantifying the effect of the target values (V_1 and V_2) and normalized distracter value ($normV_3$) on conditional choice behavior across the aggregate population data. This analysis showed that choice of the better target depended on the values of the target options, consistent with value-guided decision making ($\beta_1 = 0.88$, $P = 1.2 \times 10^{-52}$; $\beta_2 = -1.01$, $P = 4.5 \times 10^{-58}$); the larger the difference in the value of the two targets, the more likely the subject was to choose the better target. More importantly, the likelihood that a subject chose the best target depended significantly on the value of the distracter, with target choice decreasing as distracter value increased ($\beta_3 = -0.42$, $P = 2.1 \times 10^{-7}$).

In addition to the general decrease in choice efficiency with rising distracter value, model simulations predicted a biphasic response at high distracter value. To examine this in detail, we fit logistic choice functions to the population data, segregated by normalized distracter value. This analysis revealed a clear biphasic profile in empirical context dependence (Fig. 5*C*): The logistic slope parameter consistently decreased for the majority of the range of distracter values ($normV_3$ 0–0.8) but increased as distracter values approached the value of the target pairs ($normV_3$ 0.8–1.0). Fig. 5*D* plots the effective choice functions corresponding to these fits (distracter value range 0.0–0.8 shown for clarity). We confirmed this biphasic effect by repeating the generalized linear regression on low- versus high-valued distracters: Low distracter values ($normV_3 < 0.8$) decreased the efficiency of target choice ($\beta_3 = -0.54$, $P = 1.2 \times 10^{-8}$), whereas sufficiently high distracter values ($normV_3 > 0.8$) had the

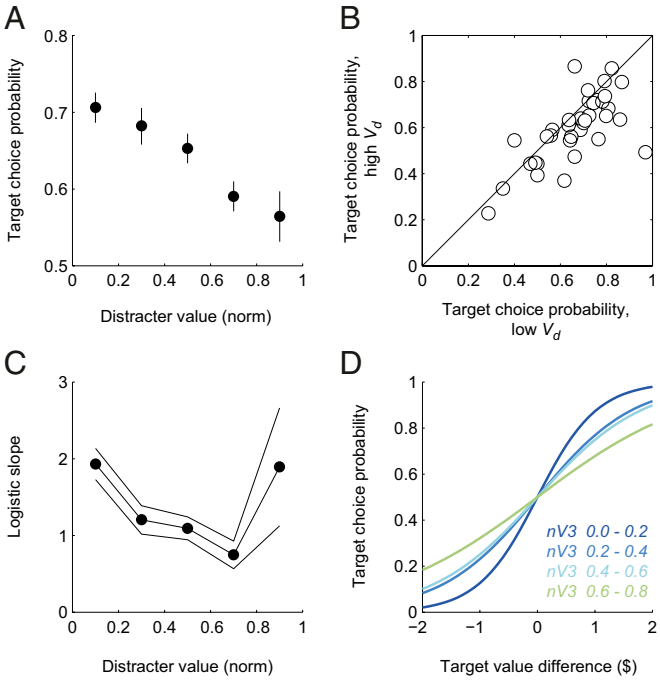

Fig. 5. Context dependence in human value-guided choice. (*A*) Choice behavior varies with distracter value. Points show relative choice probability of the higher-value target as a function of normalized distracter value averaged across the subject population (error bars, binomial CI). Target choice probability is significantly dependent on distracter value ($r = -0.80$, $P = 0.006$). (*B*) Individual subject choice behavior depends on distracter value. Each point shows the average relative choice of the better target option in high- versus low-distracter-value trials. Individual subjects' choices were classified as high or low according to normalized distracter value. (*C*) Biphasic effect on choice efficiency. Points show the population logistic function slope parameter as a function of normalized distracter value (lines, 95% CI of the parameter estimation). (*D*) Context-dependent choice curves. Curves show logistic functions fit to the population data, color-coded by distracter value for the range of decreasing efficiency (0–0.8). As distracter value initially increases from low magnitudes, the choice functions grow shallower and choice grows increasingly inefficient.

opposite effect ($\beta_3 = 0.42$, $P = 0.001$). In simulation, this increase in relative choice at high distracters is driven by the selective competition between the distracter and lower-valued target; consistent with this mechanism, distracters are chosen much more frequently when distracter value increases choice inefficiency ($normV_3 < 0.8$: 4.3%; $normV_3 > 0.8$: 20.0%).

Discussion

Context-dependent choice behavior is of particular interest in economics because it violates one of the fundamental assumptions of many rational-choice theories, namely, that decisions reflect absolute valuations assigned to individual options. The predominant examples of context-dependent choice behavior involve attribute-based decisions, where the exact nature of the effect depends on the relative position of the options in multidimensional attribute space (26, 27, 33). Although various mechanisms have been proposed for such effects (34, 35), these models typically rely on higher cognitive processes, such as attentional switching between dimensions or differential weighting of attributes, as explanations. Our results provide a different mechanism for context dependence that arises from the fundamental nature of value representation in the neural circuits implementing the decision process. We have not attempted to specifically address multiattribute context phenomena here; such effects likely involve higher-order processing in areas such as prefrontal cortex and are beyond the current scope of our model. However, we note that related normalization processes in circuits coding for specific attributes may play an important role (36).

These findings demonstrate context-dependent choice driven by the values of the choice options alone. Moreover, the biphasic nature of the contextual influence argues for careful consideration of the underlying valuations when examining such effects: At low values, distracters decrease target choice efficiency via normalization; however, at higher values, distracters increase efficiency by being selected, reducing or even reversing the overall effect. In addition to trinary-choice effects, the normalization model predicts a decrement in choice inefficiency with increasing set size, a well-documented phenomenon in behavioral experiments and empirical data (37–39). Although limitations in information processing capacity and potential postchoice dissatisfaction may be involved, the normalization model predicts that set-size effects can arise directly from the nature of the neural representation of value.

Our results suggest that normalized value coding in decision circuits has a direct influence on choice behavior. In the lateral intraparietal area (LIP), neurons represent saccade value in a normalized form, relative to the values of all available saccades (17, 19). Reach-related neurons in dorsal premotor cortex also encode a relative value representation across potential actions (18), suggesting a similar value coding in other effector systems. Moreover, normalization across option values is consistent with a number of other previous neurophysiological studies. In perceptual decision-making tasks, the activity of LIP neurons covaries with the accumulated sensory evidence (40, 41) and has been proposed to reflect the logarithm of the likelihood ratio (logLR) favoring a particular outcome (42). With fixed rewards, relative value varies monotonically with logLR, suggesting that probabilistic information can be implemented via a divisive normalization computation. Consistent with the predicted effect of set size, LIP neurons recorded during perceptual decision making show lower activity during target presentation and motion viewing with four targets versus two targets (43); a similar mechanism may underlie the effect of choice set size and target uncertainty in the superior colliculus (44, 45).

In our model, context dependence arises from two critical elements: normalization and stochasticity in value representation. Normalization during decision making drives a rescaling of neural activity driven by the value of all choice options, implementing a relative value code. Although we included a semisaturation term in the normalization algorithm to match neurophysiological observations, this parameter is not required for context dependence (*SI Results*); the crucial term is the value summation in the normalization denominator. In addition to normalization to the immediate choice set, the brain also displays normalization to the recent history of rewards (46–48). In theory, temporal normalization can also generate context dependence (29), but the consequences of such adaptation in value coding and potential interaction with choice circuit normalization remain currently unknown. Importantly, the normalization model provides a testable hypothesis of causality: Disrupting value normalization should reduce the magnitude of context-dependent choice inefficiency. Although the biophysical basis of value normalization has not been identified, potential candidate mechanisms such as feedforward or feedback inhibition offer attractive targets for further research. In our simulations, noise is also required for context dependence, mediating changing stochasticity as firing rates are scaled by normalization; notably, significant effects were observed with both rate-dependent and fixed variability. Given the importance of neural variability in our model and evidence that such variability can be strongly modulated (49), examining the nature of noisy neural codes in decision making is an important area for future work.

In summary, we report here a class of anomalous choice behavior predicted by a normalization-based decision model and confirmed in empirical choice data. This neural choice model derived from physiological measurements makes validated economic predictions, including context dependence independent of attribute-based choice and contextual set-size effects. These findings suggest that the divisive scaling documented in value coding plays a critical functional role in decision making and underscore the importance of incorporating normalization processes in the interpretation of decision-making activity and behavior.

Materials and Methods

Model. To obtain divisively normalized relative value coding, the mean firing rate μ_i representing each option was calculated from Eq. **2**. This fully parameterized relative value code replicates the normalized functional form observed in parietal recordings (17) but reduces with the appropriate parameter settings to an absolute value code ($\sigma_H = 1$, $w = 0$). Note that the full neurophysiological model originally included a baseline parameter to accommodate situations with no target in the receptive field; because this parameter is empirically small and does not apply to the choice situations examined here, it has been omitted for the sake of simplicity. For the primary analyses using normalized value codes, K was set to produce firing rates of 75 sp/s with a single option choice set; using different gain terms results in qualitatively similar results. The semisaturation constant σ_H was set to a fixed value of 50 for the primary simulations, but the specific effects of varying this parameter was explored in further simulations.

To introduce variability, two sources of noise were added independently to each mean firing rate to obtain an option value for each alternative:

$$O_i = \mu_i + \varepsilon_f + \varepsilon_s$$

$$\text{where } \varepsilon_f \sim N\left(0, \sigma^2_{fixed}\right), \ \ \varepsilon_s \sim N(0, S\mu_i).$$

ε_f implements fixed noise and is drawn from a zero-mean normal distribution with a fixed variance σ^2_{fixed}, independent of mean firing rate. ε_s implements mean-scaled noise and is drawn from a zero-mean normal distribution with a variance that is linearly dependent on the mean firing rate, where the parameter S controls how the variance scales with the mean. The effects of noise on choice behavior were examined by independently varying the parameters σ^2_{fixed} and S.

Simulation Conditions and Analysis. To examine the effect of distracter value, we simulated trinary-choice behavior between two target items (V_1 = {100, 110, . . ., 200} and V_2 = 150) and a distracter item (V_3 = {0, 20, . . ., 200}). In these simulations, value is dimensionless and the gain term K controls the magnitude of the mean firing rates. For the relative value simulations, K was set to 100 sp/s to produce realistic mean firing rates.

Relative choice behavior was quantified as the conditional choice probability of option 1 over option 2 when either is chosen:

$$p_{1|1,2} = \frac{c_1}{c_1 + c_2},$$

where c_1 and c_2 indicate the absolute number of choices for options 1 and 2, respectively. To quantify choice stochasticity, we calculated the average efficiency (E) for each choice function over all V_1 and V_2 options, where

$$E(V_1, V_2) = \begin{cases} p_{1|1,2} & \text{if } V_1 > V_2 \\ 1 - p_{1|1,2} & \text{if } V_1 < V_2. \end{cases}$$

Note that E varies inversely with stochasticity and ranges from 0.5 (random chooser) to 1 (perfect chooser) and ignores conditions where $V_1 = V_2$. To quantify normalization-driven changes in context dependence, we calculated the magnitude of the decrement in average efficiency ($-\Delta E$) between low- ($V_3 = 0$) and high- ($V_3 = 100$) valued distracters.

Human Choice Behavior Experiment. Forty healthy volunteers (21 female, ages 18–43 y) with normal or corrected-to-normal vision participated in the experiment after giving informed consent. All procedures were approved by the University Committee on Activities Involving Human Subjects of New York University. Subjects were instructed to fast for 4 h before the experimental session and informed that they would have to remain for 1 h after the completion of the session, during which the only food they could consume was any food items received from the experiment. In addition, they were instructed that one trial would be randomly selected from all of the trials in the experiment for realization at the end of the experiment, and they received a detailed explanation of the auction procedure for realization. Each subject was initially endowed with $4 for use in the bid trials. *SI Materials and Methods* gives a full description of task and realization procedures.

Choice Behavior Analysis. To examine the effect of distracter value on choice behavior across different subjects with different ranges of bid prices, we quantified a normalized distracter value:

$$normV_3 = \frac{V_3}{mean(V_1, V_2)},$$

where V_1, V_2, and V_3 are the mean bid values for the high target, low target, and distracter items in a given trial, respectively. This metric ranges from 0 to 1 and allows comparison of distracter values across subjects for population analyses. To quantify the effect of value on conditional choice data, we performed a generalized linear regression on data from the trials in which either target was chosen (n = 9,381 trials). Regression was performed using the binomial distribution and a logit link function; predictors were the values of the two target options and the normalized value of the distracter option.

ACKNOWLEDGMENTS. We thank R. Webb for helpful discussions and E. Ryklin, S. Shaw, and N. Rosenbaum for technical support. This work was supported by US Army Research Laboratory and US Army Research Office Grant W911NF-11-1-0482.

1. Heeger DJ (1992) Normalization of cell responses in cat striate cortex. *Vis Neurosci* 9(2):181–197.
2. Shapley RM, Victor JD (1978) The effect of contrast on the transfer properties of cat retinal ganglion cells. *J Physiol* 285:275–298.
3. Bonin V, Mante V, Carandini M (2005) The suppressive field of neurons in lateral geniculate nucleus. *J Neurosci* 25(47):10844–10856.
4. Britten KH, Heuer HW (1999) Spatial summation in the receptive fields of MT neurons. *J Neurosci* 19(12):5074–5084.
5. Rust NC, Mante V, Simoncelli EP, Movshon JA (2006) How MT cells analyze the motion of visual patterns. *Nat Neurosci* 9(11):1421–1431.
6. Zoccolan D, Cox DD, DiCarlo JJ (2005) Multiple object response normalization in monkey inferotemporal cortex. *J Neurosci* 25(36):8150–8164.
7. Rabinowitz NC, Willmore BD, Schnupp JW, King AJ (2011) Contrast gain control in auditory cortex. *Neuron* 70(6):1178–1191.
8. Ohshiro T, Angelaki DE, DeAngelis GC (2011) A normalization model of multisensory integration. *Nat Neurosci* 14(6):775–782.
9. Reynolds JH, Heeger DJ (2009) The normalization model of attention. *Neuron* 61(2): 168–185.
10. Simoncelli EP, Heeger DJ (1998) A model of neuronal responses in visual area MT. *Vision Res* 38(5):743–761.
11. Schwartz O, Simoncelli EP (2001) Natural signal statistics and sensory gain control. *Nat Neurosci* 4(8):819–825.
12. Carandini M, Heeger DJ (2012) Normalization as a canonical neural computation. *Nat Rev Neurosci* 13(1):51–62.
13. Louie K, Glimcher PW (2010) Separating value from choice: Delay discounting activity in the lateral intraparietal area. *J Neurosci* 30(16):5498–5507.
14. Platt ML, Glimcher PW (1999) Neural correlates of decision variables in parietal cortex. *Nature* 400(6741):233–238.
15. Sugrue LP, Corrado GS, Newsome WT (2004) Matching behavior and the representation of value in the parietal cortex. *Science* 304(5678):1782–1787.
16. Roesch MR, Olson CR (2003) Impact of expected reward on neuronal activity in prefrontal cortex, frontal and supplementary eye fields and premotor cortex. *J Neurophysiol* 90(3):1766–1789.
17. Louie K, Grattan LE, Glimcher PW (2011) Reward value-based gain control: Divisive normalization in parietal cortex. *J Neurosci* 31(29):10627–10639.
18. Pastor-Bernier A, Cisek P (2011) Neural correlates of biased competition in premotor cortex. *J Neurosci* 31(19):7083–7088.
19. Rorie AE, Gao J, McClelland JL, Newsome WT (2010) Integration of sensory and reward information during perceptual decision-making in lateral intraparietal cortex (LIP) of the macaque monkey. *PLoS ONE* 5(2):e9308.
20. Cavanaugh JR, Bair W, Movshon JA (2002) Selectivity and spatial distribution of signals from the receptive field surround in macaque V1 neurons. *J Neurophysiol* 88(5): 2547–2556.
21. Samuelson PA (1947) *Foundations of Economic Analysis* (Harvard Univ Press, Cambridge, MA).
22. Stephens DW, Krebs JR (1986) *Foraging Theory* (Princeton Univ Press, Princeton, NJ).
23. Luce RD (1959) *Individual Choice Behavior: A Theoretical Analysis* (Wiley, New York).
24. Shafir S, Waite TA, Smith BH (2002) Context-dependent violations of rational choice in honeybees (Apis mellifera) and gray jays (Perisoreus canadensis). *Behav Ecol Sociobiol* 51(2):180–187.
25. Bateson M, Healy SD, Hurly TA (2003) Context-dependent foraging decisions in rufous hummingbirds. *Proc Biol Sci* 270(1521):1271–1276.
26. Tversky A (1972) Elimination by aspects — A theory of choice. *Psychol Rev* 79(4):281.
27. Huber J, Payne JW, Puto C (1982) Adding asymmetrically dominated alternatives: Violations of regularity and the similarity hypothesis. *J Consum Res* 9(1):90–98.
28. Simonson I (1989) Choice based on reasons: The case of attraction and compromise effects. *J Consum Res* 16(2):158–174.
29. Rangel A, Clithero JA (2012) Value normalization in decision making: Theory and evidence. *Curr Opin Neurobiol* 22(6):970–981.
30. Shadlen MN, Newsome WT (1998) The variable discharge of cortical neurons: Implications for connectivity, computation, and information coding. *J Neurosci* 18(10): 3870–3896.
31. Tolhurst DJ, Movshon JA, Dean AF (1983) The statistical reliability of signals in single neurons in cat and monkey visual cortex. *Vision Res* 23(8):775–785.
32. Becker GM, DeGroot MH, Marschak J (1964) Measuring utility by a single-response sequential method. *Behav Sci* 9(3):226–232.
33. Tversky A, Simonson I (1993) Context-dependent preferences. *Manage Sci* 39(10): 1179–1189.
34. Roe RM, Busemeyer JR, Townsend JT (2001) Multialternative decision field theory: a dynamic connectionist model of decision making. *Psychol Rev* 108(2):370–392.
35. Usher M, McClelland JL (2004) Loss aversion and inhibition in dynamical models of multialternative choice. *Psychol Rev* 111(3):757–769.
36. Soltani A, De Martino B, Camerer C (2012) A range-normalization model of context-dependent choice: A new model and evidence. *PLOS Comput Biol* 8(7):e1002607.
37. Iyengar SS, Lepper MR (2000) When choice is demotivating: Can one desire too much of a good thing? *J Pers Soc Psychol* 79(6):995–1006.
38. DeShazo JR, Fermo G (2002) Designing choice sets for stated preference methods: The effects of complexity on choice consistency. *J Environ Econ Manage* 44(1):123–143.
39. Iyengar SS, Jiang W, Huberman G (2004) How much choice is too much: Determinants of individual contributions in 401K retirement plans. *Pension Design and Structure: New Lessons from Behavioral Finance*, eds Mitchell OS, Utkus S (Oxford Univ Press, Oxford), pp 83–97.
40. Roitman JD, Shadlen MN (2002) Response of neurons in the lateral intraparietal area during a combined visual discrimination reaction time task. *J Neurosci* 22(21): 9475–9489.
41. Shadlen MN, Newsome WT (2001) Neural basis of a perceptual decision in the parietal cortex (area LIP) of the rhesus monkey. *J Neurophysiol* 86(4):1916–1936.
42. Yang T, Shadlen MN (2007) Probabilistic reasoning by neurons. *Nature* 447(7148): 1075–1080.
43. Churchland AK, Kiani R, Shadlen MN (2008) Decision-making with multiple alternatives. *Nat Neurosci* 11(6):693–702.
44. Basso MA, Wurtz RH (1997) Modulation of neuronal activity by target uncertainty. *Nature* 389(6646):66–69.
45. Basso MA, Wurtz RH (1998) Modulation of neuronal activity in superior colliculus by changes in target probability. *J Neurosci* 18(18):7519–7534.
46. Tobler PN, Fiorillo CD, Schultz W (2005) Adaptive coding of reward value by dopamine neurons. *Science* 307(5715):1642–1645.
47. Padoa-Schioppa C (2009) Range-adapting representation of economic value in the orbitofrontal cortex. *J Neurosci* 29(44):14004–14014.
48. Kobayashi S, Pinto de Carvalho O, Schultz W (2010) Adaptation of reward sensitivity in orbitofrontal neurons. *J Neurosci* 30(2):534–544.
49. Churchland MM, et al. (2010) Stimulus onset quenches neural variability: A widespread cortical phenomenon. *Nat Neurosci* 13(3):369–378.

Supporting Information

Louie et al. 10.1073/pnas.1217854110

SI Results

Effect of Neural Variability on Model Context Dependence. To examine the role of variability, we examined choice across a range of fixed and mean-scaled noise levels and quantified the decrease in efficiency mediated by increasing distracter value ($-\Delta E$; decrease in optimal choice between $V_3 = 0$ and $V_3 = 100$). These simulations revealed three properties governing the influence of variability on context dependence (Fig. S1). First, noise of either kind is critical to context-dependent behavior: Without trial-to-trial variability in the representation of value, discriminability between options is unaffected by the shift in mean firing rates produced by divisive scaling. This effect is unsurprising given that stochastic choice behavior in the model depends on neural noise, but it emphasizes the importance of understanding the role of variability in neural coding. Second, context dependence occurs across a broad range of both fixed and mean-scaled noise levels. To orient the reader, we point out that an ideal Poisson neuron is represented by $S = 1.0$ and $\sigma_{fixed} = 0$. Finally, distributional noise characteristics are important: Context dependence consistently decreases with the strength of the mean-scaled noise relationship (S). With mean-scaled variance, the widths of the firing-rate distributions decrease as rates are reduced by divisive scaling, partially compensating for decreases in mean rate differences driven by normalization.

Effect of the Semisaturation Constant on Model Context Dependence. In addition to divisive scaling, the behavior of the normalization algorithm is governed by the semisaturation term σ_H, which controls the effective response range and saturation behavior. With a single option, σ_H determines the value V_i that produces the half-maximal response. With more than one option, σ_H functions in an additional manner, controlling the degree of context dependence in value representation (Fig. S2*A*). At low σ_H (relative to V), the denominator in Eq. **2** is dominated by the value terms and the model shows strong context dependence: The activity representing the value of option 1 depends markedly on the value of the other alternatives (Fig. S2*A Left*). At higher σ_H, the denominator is increasingly dominated by the semisaturation constant itself and the response approaches an absolute value representation (Fig. S2*A Center* and *Right*).

Given its modulatory control of contextual value coding, we hypothesized that the semisaturation constant would also affect the extent of behavioral context dependence. Fig. S2*B* shows simulated choice behavior at three different magnitudes of σ_H (10, 100, or 1,000). In these simulations, the gain parameter was adjusted to keep mean firing rates approximately equivalent; all other model parameters were fixed. As evident in the decreasing range of choice curves, a larger semisaturation constant decreases the effect of context on behavior. Examined across a broad range of σ_H magnitudes, context dependence decreases exponentially as a function of the semisaturation parameter (Fig. S2*C*); this exponential decrease suggests that context-dependent effects persist for a broad range of semisaturation values.

Thus, context dependence does not require the specific parameters of the normalization algorithm observed in parietal cortex; in particular, contextual effects are driven by the value summation term in the normalization denominator. However, inclusion of σ_H in the model allows a parametric examination of the effects of normalization terms. These results show that the extent of context dependence depends on the precise parameters of normalization and thus may be modifiable. For example, changes in σ_H have been proposed to mediate the effects of adaptation in visual responses, suggesting that the normalization mechanism (and context dependence) may vary with temporal history. In the sensory and decision-making literature, the semisaturation constant is primarily treated as an empirical constant fit to neural data; identifying the biophysical source of this term and mechanisms by which it may be modulated in neural circuits is a key area of future research.

SI Materials and Methods

Monkey Trinary-Choice Experiment. Two male rhesus monkeys (*Macaca mulatta*) were used as subjects (monkey W, ~6.0 kg; monkey B, ~14.0 kg). All experimental procedures were performed in accordance with the US Public Health Service's *Guide for the Care and Use of Laboratory Animals* and approved by the New York University Institutional Use and Care Committee.

Experiments were conducted in a dimly lit, sound-attenuated room using standard techniques. Visual stimuli were generated using an array of tristate light-emitting diodes situated on a tangent screen 145 cm from the eyes of the monkey. Eye movements were monitored using the scleral search coil technique, with horizontal and vertical eye position sampled at 500 Hz using a quadrature phase detector (Riverbend Electronics). Presentation of visual stimuli and water reinforcement delivery were controlled with an integrated software and hardware system (Gramalkn; Ryklin Software).

Each session was conducted in blocks consisting of a series of instructed trials followed by choice trials. In a given block, reward magnitudes were randomly assigned to three target locations situated 16° from fixation and equidistant from one another. To encourage the animals to learn new reward-location associations each block, one of four different location triplets was randomly selected for each block. Reward magnitudes (in microliters) were drawn in a pseudorandom fashion from the sets $V_1 = \{130, 143, 156, 169, 182\}$, $V_2 = 156$, and $V_3 = \{26, 104\}$.

Individual blocks began with 40 instructed trials. Each trial began with the monkey fixating a central fixation target (500 ms). A target was then presented in one of the three locations assigned to the block (1,500 ms). Finally, the fixation target was extinguished, and the monkey was rewarded with the designated amount for a saccade to the peripheral target within 500 ms. Instructed trials were followed by a series of choice trials (range 15–30 trials), which were identical to instructed trials except the three targets were simultaneously presented and the monkey was rewarded the amount associated with the selected target. All blocks of length 30 or fewer were included in the analysis; similar results were obtained with data restricted to smaller datasets.

Human Trinary-Choice Experiment. Each behavioral session began with 60 bid trials. In each bid trial, subjects viewed an image of a snack-food item on a computer display and reported how much they would be willing to bid for that item using a mouse-controlled slider bar; possible bid prices ranged from \$0–4 in \$0.01 increments. Stimuli depicted 30 different food items (common salty and sweet snack foods), presented as high-resolution color images (110 pixels per inch). Items were presented in randomized order, and each individual good was presented twice.

Following the bid trials, the items were automatically sorted by their mean bid values into a target group (10 highest-ranked) and a distracter group (20 lowest-ranked). Subjects then performed 250 choice trials; in each trial, subjects viewed three options (two targets and one distracter) and indicated their choice by pressing

a mouse button. Distracters comprised a subset of 10 items chosen to sample widely from the identified distracter group [items ranked 1, 3, ..., 19 in mean Becker–DeGroot–Marschak (BDM) bid]. Target item pairs were chosen to sample widely from the possible pairwise target value differences. Each distracter was presented with 25 different target pairs, and each trinary-choice set was presented only once. The location of each item on the screen (left, middle, or right) was randomly assigned in each trial. Following the completion of the session, one of the 310 trials was randomly selected for realization.

If a bid trial was selected, the outcome was determined via a BDM auction; the BDM procedure is widely used in laboratory economic studies because it is easy to explain and implement, and the optimal strategy for subjects is to report their exact subjective valuation. To realize a bid trial, subjects drew a chip from a bag containing chips numbered from \$0–\$4 in \$0.10 increments; the drawn number determined the price p of the item in that trial and was compared with the bid b. If $b \geq p$, subjects received the item for the price p; if $b < p$, the subjects paid nothing and did not receive the item. Thus, the best strategy for subjects is to report the maximal price they would be willing to pay, because this has no effect on the price itself but rather on whether or not the subjects will purchase the item. Subjects were carefully informed of this property of the BDM auction in the initial instructions and practiced it before the actual experiment. If a choice trial was selected, subjects received the food item they selected in that trial.

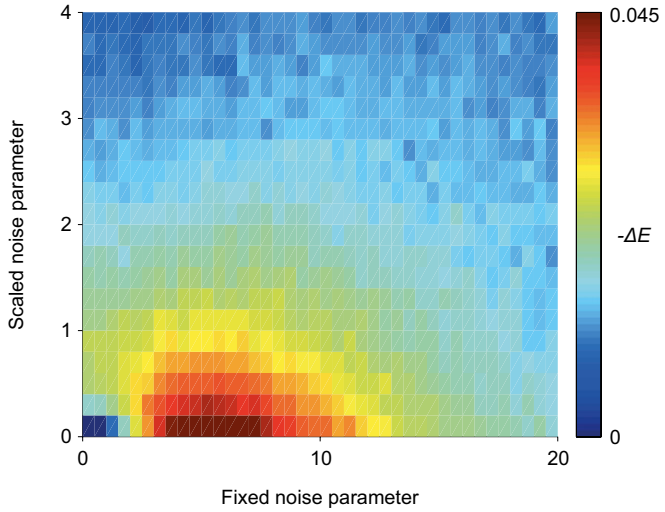

Fig. S1. Effect of variability on context dependence. Color indicates the normalization-driven decrease in choice efficiency ($-\Delta E$) as a function of two sources of noise: rate-dependent and rate-independent variability. Trinary-choice simulations were conducted and efficiency quantified as shown in Fig. 2. Data are plotted as a function of the relevant noise parameters (rate-dependent, scaling parameter S; rate-independent, fixed noise SD σ_{fixed}). Noise of either form is critical for context dependence: At minimal levels of both types of variability, changes in context do not affect choice efficiency (lower left).

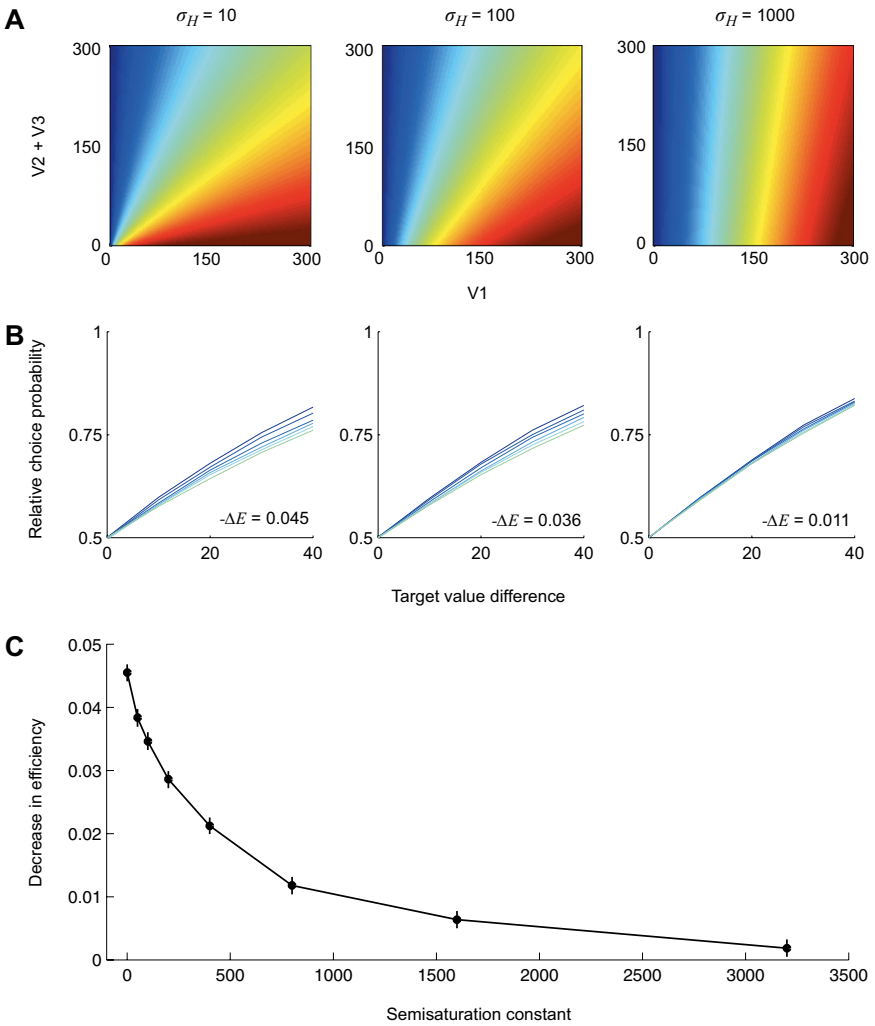

Fig. S2. Context dependence governed by the form of normalization. (*A*) Normalization model response representing option 1 as a function of its value (V_1) and the summed value of alternative targets ($V_2 + V_3$) for low, medium, and high semisaturation parameters (σ_H). Color map indicates model neuron firing rate (min = 0 sp/s, max = 75 sp/s). As σ increases, the value representation grows increasingly independent of alternative options, evident as vertical shading. (*B*) Relative target-choice curves at different semisaturation parameters, as in *A*. At higher σ_H, distracter value has a smaller effect on choice behavior. Colors indicate different distracter values as in Fig. 2; for legibility, data are shown for distracter values from 0 to 100 and positive target-value differences. (*C*) Context-driven decrease in choice efficiency ($-\Delta E$) decreases exponentially as a function of semisaturation parameter magnitude. Error bars indicate bootstrap 95% confidence intervals.

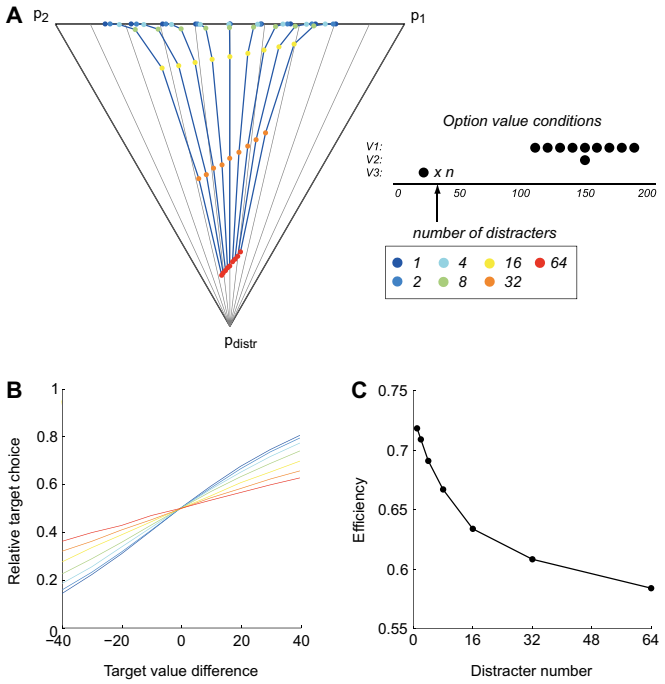

Fig. S3. Normalization model and set-size effects. (*A*) Example set size-dependent choice behavior. The value of two target options (V_1 and V_2) were varied as in the trinary-choice simulations; the number of additional, fixed-value ($V_3 = 20$) distracter items varied from 1 to 64. Each point in the simplex plot represents average choice behavior in a given set size for a particular value condition, color-coded by the number of distracters. Choice behavior under fixed target-value pairs (V_1 and V_2) are connected with blue lines and deviate markedly from the linear constant relative ratio lines predicted by rational-choice theory (gray lines). Example simulation parameters: $K = 100$, $\sigma_H = 50$, $w = 1$, $\sigma_{fixed} = 8$, $S = 0$. (*B*) Context-dependent relative target choice functions. Lines are color-coded by distracter number, as in *A*. (*C*) Relative target choice efficiency plotted as a function of distracter number.